Inorg. Chem. **2008**, *47*, 8610−8612

Single-Molecule-Magnet Behavior and Spin Changes Affected by Crystal Packing Effects

Patrick L. Feng,[†] Changhyun Koo,[‡] John J. Henderson,[§] Motohiro Nakano,[||] Stephen Hill,[‡] Enrique del Barco,[§] and David N. Hendrickson*,[†]

Department of Chemistry and Biochemistry, University of California, San Diego, La Jolla, California 92093-0358, Department of Physics, University of Florida, Gainesville, Florida 32611, Department of Physics, University of Central Florida, Orlando, Florida 32816-2385, and Division of Applied Chemistry, Osaka University, Suita, Osaka 565-0871, Japan

Received July 1, 2008

Five Mn_3Zn_2 heterometallic complexes have been synthesized and structurally and magnetically characterized. Spin ground states up to $S = 6$ have been observed for these complexes and are shown to depend on the cocrystallizing cation and on the terminal ligand. Large axial zero-field interactions ($D = -1.16$ K) are the result of near-parallel alignment of the Mn^{III} Jahn−Teller axes. High-frequency electron paramagnetic resonance, single-crystal magnetization hysteresis, and alternating current susceptibility measurements are presented to characterize $[NEt_4]_3[Mn_3Zn_2(salox)_3O(N_3)_6X_2]$ [$X^- = Cl^-$ (**1**), Br^- (**2**)] and $[AsPh_4]_3[Mn_3Zn_2(salox)_3O(N_3)_6Cl_2]$ (**3**) and reveal that **1** and **2** are single-molecule magnets ($U_{eff} = 44$ K), while **3** is not.

The observance of slow magnetization relaxation and quantum effects in single-molecule magnets (SMMs) has led to intense research interest in the area.[1−7] The basic requirements for a SMM include an appreciable spin ground state and a negative uniaxial anisotropy.[7] One synthetic strategy has been to maximize the spin by facilitating ferromagnetic interactions among anisotropic metal ions such as Mn^{3+}. Impressively large spin ground states up to $^{83}/_2$ have been achieved but have not resulted in increased barriers due to corresponding decreases in $|D|$.[8] A related approach involves maximizing the magnitude of $|D|$ while maintaining an appreciable spin. This method has been particularly successful for the synthesis of SMMs that are supported by phenolic oximes.[9−12] In fact, the largest barrier to magnetization reversal to date has been observed in the complex $[Mn_6O_2(Et\text{-}sao)_6(O_2CPh(Me)_2)_2(EtOH)_6]$ as a result of a large negative anisotropy ($D = -0.618$ K) and an $S = 12$ spin ground state.[9]

There is also significant interest in understanding the specific factors that govern ferromagnetic exchange in oxo-centered Mn_3 triangles, which serve as molecular building blocks for complexes such as Mn_6.[10,13] Variations in the Mn−N−O−Mn angle in oximate-supported complexes have been shown to affect the nature and magnitude of magnetic exchange interactions, where larger torsion angles correspond to stronger ferromagnetic interactions. These studies, however, have been based on comparisons between nonidentical Mn_3 triangles differing in coordination environment and chelating ligands.[10,13] Indeed, the $S = 12$ Mn_6 SMMs were also obtained via chemical modification of the oxime ligand.[12] Our complexes **1** and **3** have the formula $[cation]_3[Mn_3Zn_2(salox)_3O(N_3)_6X_2]$, with $X^- = Cl^-$, and switch from $S = 6$ to a strongly mixed low-spin ground state as a result of a cocrystallizing cation change from $[NEt_4]^+$ to $[AsPh_4]^+$. Likewise, complexes **2**, **4**, and **5** have $[cation]^+ = [NEt_4]^+$ and exhibit similar spin-state changes as a result

* To whom correspondence should be addressed. E-mail: dhendrickson@ucsd.edu. Fax: 858-534-5383.
[†] University of California, San Diego.
[‡] University of Florida, Gainesville.
[§] University of Central Florida.
[||] Osaka University.

(1) Sessoli, R.; Tsai, H.-L.; Schake, A. R.; Wang, S.; Vincent, J. B.; Folting, K.; Gatteschi, D.; Christou, G.; Hendrickson, D. N. *J. Am. Chem. Soc.* **1993**, *115*, 1804.
(2) Sessoli, R.; Gatteschi, D.; Caneschi, A.; Novak, M. A. *Nature* **1993**, *365*, 141.
(3) Thomas, L.; Lionti, F.; Ballou, R.; Gatteschi, D.; Sessoli, R.; Barbara, B. *Nature* **1996**, *383*, 145.
(4) Wernsdorfer, W.; Aliaga-Alcalde, N.; Hendrickson, D. N.; Christou, G. *Nature* **2002**, *416*, 406.
(5) Hill, S.; Edwards, E. S.; Aliaga-Alcalde, N.; Christou, G. *Science* **2003**, *302*, 1015.
(6) Wernsdorfer, W.; Bhaduri, S.; Boskovic, C.; Christou, G.; Hendrickson, D. N. *Phys. Rev. B* **2002**, *65*, 180403.
(7) Gatteschi, D.; Caneschi, A.; Pardi, L.; Sessoli, R. *Science* **1994**, *265*, 1054.
(8) Ako, A. M.; Hewitt, I. J.; Mereacre, V.; Clerac, R.; Wernsdorfer, W.; Anson, C. E.; Powell, A. K. *Angew. Chem., Int. Ed.* **2006**, *45*, 4926.
(9) Milios, C. J.; Vinslava, A.; Wernsdorfer, W.; Moggach, S.; Parsons, S.; Perlepes, S. P.; Christou, G.; Brechin, E. K. *J. Am. Chem. Soc.* **2007**, *129*, 2754.
(10) Cano, J.; Cauchy, T.; Ruiz, E.; Milios, C. J.; Stoumpos, C. C.; Stamatatos, T. C.; Perlepes, S. P.; Christou, G.; Brechin, E. K. *J. Chem. Soc., Dalton Trans.* **2008**, 234.
(11) Yang, C.-I.; Wernsdorfer, W.; Lee, G.-L.; Tsai, H.-L. *J. Am. Chem. Soc.* **2007**, *129*, 456.
(12) Milios, C. J.; Inglis, R.; Vinslava, A.; Bagai, R.; Wernsdorfer, W.; Parsons, S.; Perlepes, S. P.; Christou, G.; Brechin, E. K. *J. Am. Chem. Soc.* **2007**, *129*, 12505.
(13) Viciano-Chumillas, M.; Tanase, S.; Mutikainen, I.; Turpeinen, U.; de Jongh, L. J.; Reedijk, J. *Inorg. Chem.* **2008**, *47*, 5919.

10.1021/ic801208z CCC: $40.75
Published on Web 09/05/2008

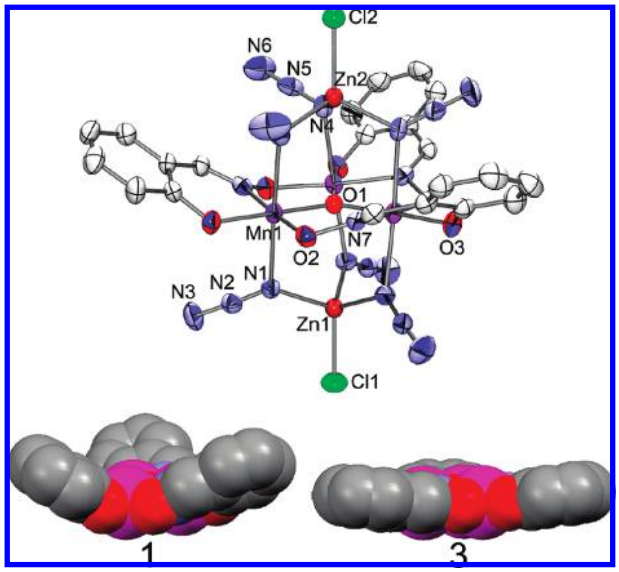

Figure 1. (top) Molecular structure of complex **1**. (bottom) Space-filling model for the $[Mn_3(salox)_3O]^+$ magnetic core of complexes **1** and **3**, when viewed in the Mn_3^{III} plane.

of a change in the terminal X^- ligand from Br^- to I^- to N_3^-, respectively. These observations highlight the importance of size and shape upon the crystal packing of these molecules and their resulting magnetic properties.

Complexes **1**−**3** crystallize in the trigonal space groups *R*3*c*, *R*3*c*, and *R*$\bar{3}$*c*, respectively, as racemic mixtures of C_3-symmetric chiral molecules. Complexes **4** and **5** do not exhibit C_3 symmetry and crystallize in the monoclinic space groups *P*21/*c* and *P*21/*n*, respectively. The metallic cores for all molecules are comprised of a μ_3-oxo-centered triangle of Mn^{3+} ions with two Zn^{2+} ions located above and below the Mn_3 plane. Magnetic exchange interactions between Mn^{3+} ions are propagated by the central μ_3-oxo ion and through the coordinating oxime. Six $\mu_{1,1}$-azido ligands bridge the Mn^{3+} ions to the two tetrahedral Zn^{2+} ions, and a terminal halide/azide binds to the axial coordination site of the Zn^{2+} ions. Complexes **1**−**3** crystallize in one molecular orientation with no solvate molecules, whereas **4** and **5** exhibit multiple molecular orientations and each cocrystallize with a MeOH solvate molecule.

Complexes **1** and **2** have large Mn−N−O−Mn torsion angles of 32.28° and 32.08°, as is also evident by the puckered phenyl ring orientation (Figure 1, bottom). This results in $S = 6$ spin ground states (vide supra) and arises from the crystal packing in the noncentrosymmetric *R*3*c* space group. The metal clusters are arranged in columns along the *c* axis, with the molecular C_3 axis (easy-axis) coinciding with the *c* axis. Adjacent molecules along the *c* axis exist as alternating stereoisomers in a "head-to-tail" arrangement, while adjacent molecules in the *a*−*b* plane are identical. $[NEt_4]^+$ cations fit into the chiral void spaces of the metal cluster and also exhibit alternating handedness when viewed along *c*.

A similar packing arrangement is not possible in **3** because the $[AsPh_4]^+$ cation is larger and does not have the same packing flexibility. Instead, complex **3** crystallizes in the centrosymmetric space group *R*$\bar{3}$*c*, where adjacent molecules along the *c* axis and *a*−*b* plane exist as different stereoisomers in the "head-to-tail" orientation. Inspection of the structure reveals a reduced Mn−N−O−Mn torsion angle of 11.93° and virtually coplanar phenyl rings (Figure 1, bottom), as enforced by the presence of bulky $[AsPh_4]^+$ cations. The result of this crystalline packing is a low-spin ground state arising from strongly mixed low-lying spin states (Figure S4 in the Supporting Information). It is also notable that the individual-ion Jahn−Teller (JT) cant angles in **3** (5.06°) are close to those of **1** (8.43°) and **2** (8.09°), indicating that the oximate ligand geometry more likely determines the nature of magnetic exchange interactions, not changes in the direction of the JT elongations.

The magnetostructural effects of terminal-ion substitution have also been investigated. In spite of the terminal-ion coordinating to diamagnetic Zn^{2+} ions, there are significant structural and magnetic effects associated with keeping the cation the same but changing the terminal ligand. Complexes **1** and **2** have Cl^- and Br^- as terminal ligands, respectively, and possess similar trigonal crystal structures and $S = 6$ ground states. Complex **4** contains the larger I^- ion and exhibits a monoclinic crystal packing and smaller torsion angles, resulting in a strongly mixed low-spin ground state. These observations may be attributed to the $[NEt_4]^+$ cation geometry with respect to the cavity formed by adjacent bridging N_3^- ions and the terminal halide. Complexes **1** and **2** have smaller halide groups and a larger void space for an ethyl fragment to fit, when compared to **4**. Further crystal packing differences are evident from the lower site symmetry and nonaxially symmetric orientation of terminal ligands in **4**.

A related situation is observed for complex **5**, where bent terminal N_3^- ligands prevent C_3 symmetry and require a lower-symmetry space group. The resulting monoclinic crystal packing exhibits small Mn−N−O−Mn angles and leads to an $S = 2$ ground state (Figure S6 in the Supporting Information).

In addition to the above structural analysis, magnetic susceptibility data were collected on complexes **1**−**5** from 300 to 1.8 K and from 0.01 to 5 T. These data were fit via block diagonalization of the microscopic spin Hamiltonian schematized by eq 1 and explicitly defined in Figure S1 in the Supporting Information.[14]

$$\hat{H} = \hat{H}_{\text{exchange}} + \hat{H}_{\text{zfs}} + \hat{H}_{\text{Zeeman}} \quad (1)$$

These data were fit by means of an uncoupled basis set for three Mn^{III} ions (125 × 125 Hamiltonian matrix), yielding best-fit parameters for complex **1** of $g = 1.93$, $J_{\text{Mn-Mn}} = +2.44$ K, and $D_{\text{Mn}^{III}} = -4.76$ K; the $\theta = 8.43°$ single-ion JT cant angles were also taken into account. Zero-field-splitting (zfs) parameters *D* and B_4^0 for a molecular $S = 6$ ground state were then extracted from the eigenvalue spectrum of the microscopic Hamiltonian for complex **1**, resulting in values of $D = -1.192(9)$ K and $B_4^0 = -1.110(3) \times 10^{-4}$ K (Figure S2 in the Supporting Information). In comparison, the low-spin complex **3** could not be approximated by the giant spin Hamiltonian because of low-

(14) Wilson, A.; Lawrence, J.; Yang, E.-C.; Nakano, M.; Hendrickson, D. N.; Hill, S. *Phys. Rev. B* **2006**, *74*, 140403.

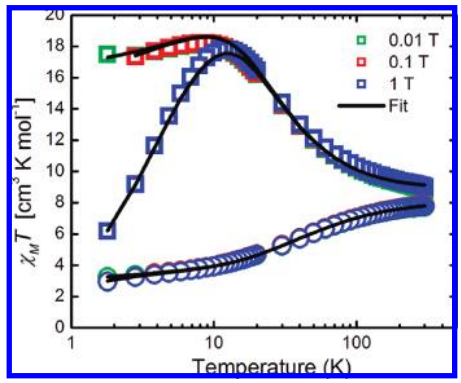

Figure 2. Fit of $\chi_M T$ vs T data for complexes **1** (squares) and **3** (circles), taken at 0.01, 0.1, and 1 T from 300 to 1.8 K. Fitting parameters are described in the text.

lying excited states. The best-fit single-ion parameters for complex **3** were determined as $g = 1.94$, $J_{Mn-Mn} = -4.07$ K, $D_{Mn^{III}} = -6.20$ K, and $\theta = 5.06°$. Additional magnetic data and fits are provided in the Supporting Information.

Alternating current (ac) susceptibility measurements were taken between 10 and 1000 Hz and from 1.8 to 5 K for complexes **1**−**5**. Clear peaks in the out-of-phase susceptibility were observed for **1** and **2** and indicate slow relaxation of a SMM (Figure S7 in the Supporting Information). Fitting to the Arrhenius equation resulted in a magnetization reversal barrier of $U_{eff} = 44$ and 46 K for **1** and **2**, respectively. No out-of-phase ac susceptibility signal was observed for complexes **3**−**5**.

High-frequency electron paramagnetic resonance (HFEPR) measurements were taken on a single crystal of **1** to directly probe the transitions between spin states and more accurately determine the spin Hamiltonian parameters. Very sharp absorption peaks were observed and indicate a monodisperse crystalline environment and a very small distribution of local microenvironments. Furthermore, a single molecular orientation made it possible to apply the field precisely along the molecular easy-axis and hard-plane. Variable-temperature spectra for the hard-plane orientation are given in Figure 3 and confirm a large negative value of the axial zfs parameter D. Exceptional simulations of the easy-axis and hard-plane multifrequency data gave the following unique parameter set: $g_z = 1.97(2)$, $g_x = g_y = 1.96(2)$, $D = -1.16(1)$ K, and $B_4^0 = -7.6(5) \times 10^{-5}$ K. No measurable transverse anisotropy was detected in these initial studies.

HFEPR experiments on complex **2** yielded spectra and simulation parameters similar to those of **1**, while a broad transition peak was observed for complex **3**. The observance of a broad peak is consistent with the strongly mixed spin states in **3**.

Magnetization hysteresis measurements were conducted on a single crystal of **1** using micro-Hall-bar probe magnetometry, with the field applied along the molecular easy axis. The resulting hysteresis loop is shown in Figure 4 and is characteristic of a SMM, i.e., sharp vertical steps corresponding to quantum tunneling of the magnetization (QTM). The sharp QTM steps reflect the single molecular orientation, an absence of solvate molecules, and high crystal quality. The QTM step positions are in excellent agreement with the

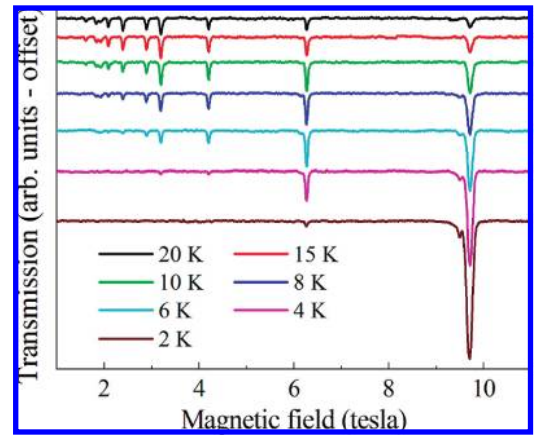

Figure 3. Hard-plane variable-temperature HFEPR for an oriented single crystal of **1**, taken at 104.1 GHz from 2 to 20 K.

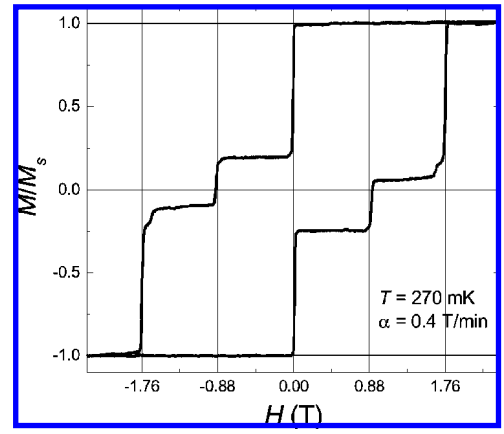

Figure 4. Hysteresis loop measurement for a single crystal of **1**. The magnetization is normalized by the saturation value M_S.

zfs parameters obtained from magnetization fitting and HFEPR. Similar hysteresis data were found for **2**.

A series of closely related Mn_3Zn_2 complexes have been synthesized and shown to undergo spin-state changes as a result of changes in the cocrystallizing cation and terminal ligand. These reactions produce well-formed crystalline products in high yields (75−90%) and provide an unprecedented platform from which to study the origins of ferromagnetic exchange in Mn_3 triangles with chemically identical magnetic cores. Investigations are underway to elucidate the synthetic requirements for tuning the magnetic properties of new structures based on these triangular Mn_3 subunits.

Acknowledgment. This work was supported by the National Science Foundation.

Supporting Information Available: Experimental details, crystallographic information in CIF format, fits of dc susceptibility data, and ac susceptibility data. This material is available free of charge via the Internet at http://pubs.acs.org. The atomic coordinates for these structures (CCDC 692288, 692289, 699692, 699694, 699695) have been deposited with the Cambridge Crystallographic Data Centre. The coordinates can be obtained, upon request, from the Director, Cambridge Crystallographic Data Centre, 12 Union Road, Cambridge CB2 1EZ, U.K.

IC801208Z